



Cite this: *New J. Chem.*, 2019, 43, 16218

Received 11th July 2019,
Accepted 18th September 2019

DOI: 10.1039/c9nj03574e

rs.c.li/njc

Counter-complementarity control of the weak exchange interaction in a bent $\{\text{Ni(II)}_3\}$ complex with a μ -phenoxide- μ -carboxylate double bridge†

Guillermo Fiorini,^a Luca Carrella,^b Eva Rentschler ^b and Pablo Alborés ^{*a}

We have prepared and structurally characterized a novel $\{\text{Ni}_3\}$ bent complex bearing a double μ -phenoxide- μ -carboxylate bridge. Both terminal Ni(II) sites are symmetry related, offering a simplified exchange interaction scheme. DC magnetic data is consistent with a weak antiferromagnetic interaction between the central and terminal Ni(II) ions. As expected for a Ni(II) system, local zero-field splitting is observed, which can be experimentally established. Broken symmetry quantum chemical calculations, as well as *ab initio* CASSCF-SA-SOC computations that support the magnetic experimental data, were also performed. From the analysis of other reported closely related Ni(II) systems, a counter-complementarity effect exerted by the carboxylate bridge is proposed, which might explain the weaker exchange interactions compared to those observed in double μ -phenoxide bridged Ni(II) compounds.

Introduction

The research field of molecular magnetism is envisaged as being a key area in the exploration of the diversity of systems, with the aim of understanding the origins and the degree of strength of the spin exchange interaction.¹ Regarding this fundamental issue, several magneto-structural correlations (both theoretical and experimental) have been established² and owing to these studies, a broad range of molecule-based magnetic materials including single-molecule-magnets, have been reported in recent years. With respect to the exchange interaction in the polynuclear compounds of paramagnetic metal ions, the ferromagnetic type is significantly rarer than the anti-ferromagnetic one.

The preparation of coordination compounds exhibiting ferromagnetic exchange interactions constitutes a hard task for synthetic chemists, particularly when dealing with systems with a high degree of nuclearity. The importance of succeeding in this enterprise relies not only on the scarcity of systems with dominant ferromagnetic exchanges, but also in the fact that a high spin is required, together with a large axial anisotropy, in

order to achieve molecular nanomagnets.³ There are different alternatives for the development of ferromagnetic exchange interactions, the main ones being orthogonality of the magnetic orbitals, spin-polarization or counter-complementarity of the bridging ligands.⁴ In this sense, cumulated experimental information indicates that there is not a definitive recipe to find a bridging ligand that unequivocally promotes the ferromagnetic exchange interaction independent of the metal ion and the nature of additional bridges.

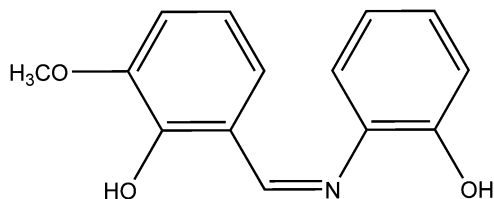
It is well established that the counter-complementarity effects of a second bridging ligand (L) play a fundamental role in governing the magnetic properties of heterobridged μ -hydroxo/alkoxo/phenoxo- μ -L Cu(II) dinuclear complexes (L = azide, thiocyanate, pyrazolate, carboxylate, *etc.*).⁴ Although Cu(II) has one magnetic orbital, other 3d metal ions (*e.g.* Ni(II), Mn(II) and Fe(II)) have two or more magnetic orbitals. Hence, it becomes very challenging to explore counter-complementarity effects in these systems owing to the many possible combinations of magnetic orbitals. The Ni(II) ion with only two unpaired electrons (two magnetic orbitals) appears to be the simplest case after the Cu(II) ones. In this sense, focusing on the dinuclear or trinuclear compounds (with high symmetry) of Ni(II) offers the possibility of looking into the nature of the exchange interaction mediated by the hetero-bridged motifs.

In this work, we report a novel Ni(II) trinuclear complex arranged in a bent configuration with symmetry related Ni(II) terminal sites, bearing a μ -phenoxo- μ -carboxylate bridge, with the formula $[\text{Ni}_3^{\text{II}}(\text{L}_2)(\text{piv})_2(\text{H}_2\text{O})_4]$ (**1**), $\text{H}_2\text{L} = o$ -aminophenol/*o*-vanillin Schiff base (Scheme 1), Hpiv = pivalic acid. The ligand H_2L has been previously employed to fabricate different Ni(II)

^a Departamento de Química Inorgánica, Analítica y Química Física/INQUIMAE (CONICET), Facultad de Ciencias Exactas y Naturales Universidad de Buenos Aires, Pabellón 2, Ciudad Universitaria, C1428EHA Buenos Aires, Argentina. E-mail: albores@qi.fcen.uba.ar; Fax: +54-11-4576-3341

^b Johannes Gutenberg University Mainz Chemistry, Institute of Inorganic and Analytical Chemistry, Duesbergweg 10-12, 55128 Mainz, Germany

† Electronic supplementary information (ESI) available. CCDC 1938756. For ESI and crystallographic data in CIF or other electronic format see DOI: 10.1039/c9nj03574e



Scheme 1 The Schiff-base type H_2L ligand employed for the synthesis of complex **1**.

complexes, as well as $Ni(II)/Ln(III)$ compounds with a variety of nuclearities.⁵

Through a combined experimental and theoretical approach, we attempt to understand the weak exchange interactions observed in complex **1**, close to the boundary between a ferro/antiferromagnetic nature.

Results and discussion

Synthesis and structural characterization

The reaction of stoichiometric amounts of a dinuclear $Ni(II)$ pivalate precursor with the Schiff-base type H_2L ligand in acetonitrile under mild conditions affords single crystal crops with high reproducibility. X-ray data show that these crystals correspond to the trinuclear $Ni(II)$ complex **1** (Fig. 1).

It packs into the monoclinic $C_{2/c}$ space group with one acetonitrile solvent molecule and two pivalic acid molecules per molecule of complex **1** (Fig. S1, ESI[†]). A crystallographic imposed C_2 rotation axis makes both the terminal $Ni(II)$ units

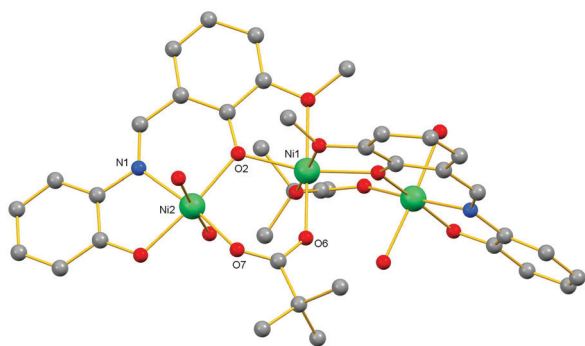


Fig. 1 A ball and stick molecular representation of the crystal structure of complex **1**. H atoms have been removed for clarity. Colour code: Green: Ni; red: O; blue: N; grey: C.

strictly equivalent. The trinuclear $Ni(II)$ complex shows a bent arrangement with a $Ni-Ni-Ni$ angle of $146.27(4)^\circ$. All of the $Ni(II)$ centres display distorted octahedral coordination environments with O_5N and O_6 ligands for the terminal and central $Ni(II)$ centres, respectively. Terminal $Ni(II)$ sites are chelated by the L^{2-} ligand, and doubly bridged to the central $Ni(II)$ centre through the phenoxide O of the L^{2-} ligand and a *syn-syn* pivalate ligand. Two water ligands complete their coordination sphere. The $Ni(II)-O$ bond distances involving water ligands are the longest, $2.088(4)$ and $2.129(5)$ Å, with the remaining $Ni(II)-O/Ni(II)-N$ bond distances ranging from $2.031(4)$ – $2.050(4)$ Å. These metric data suggest an axial distortion running along the $O-Ni-O$ axis (both O atoms from water ligands). On the other hand, the central $Ni(II)$ site is chelated twice by the phenoxide-methoxy motif of the L^{2-} ligand in a *cis* arrangement. The coordination sphere is completed by both bridging pivalate ligands. Owing to the imposed crystal symmetry, the central $Ni(II)$ $Ni-O$ bond distances are grouped in three equivalent pairs corresponding to the contiguous bonds: $2.014(4)$, $2.030(3)$ and $2.110(4)$ Å. The longest pair of bond distances, as expected, corresponds to the $Ni-O$ bond involving the L^{2-} ligand methoxy group. This bonding pattern indicates a trigonal distortion instead of an axial one. Owing to the planar arrangement of the L^{2-} ligands, the elongated $O-Ni-O$ axis (the one involving both water ligands) of the terminal $Ni(II)$ sites, makes an angle of $70.8(2)$ degrees (estimated through the $O(4)-Ni(2)-Ni(2')-O(4')$ torsion angle), running close to a perpendicular arrangement.

Surprisingly, few structural characterized $\{Ni_3\}$ complexes sharing the $\mu-OR/\mu-syn$, *syn*-carboxylato bridge, have been reported so far. The Cambridge Structural Database (CSD)⁶ only affords six structures, most of them built upon rather similar Schiff-base like ligands as H_2L (see Table 1).⁷ The structural similarity of these complexes, all showing the bent $\{Ni_3\}$ motif, affords a range of $Ni-Ni-Ni$ angles from *ca.* 130 to 150° .

The coordinated water ligands are involved in hydrogen bridge interactions that are intra-molecular and inter-molecular in nature, with μ -pivalate ligands in the case of the former and free pivalic acid molecules together with the O-phenoxide atoms of the L^{2-} ligand of the neighbouring complex in the latter (Fig. S2, S3 and Table S2, ESI[†]). The free pivalic acid molecule in the packing is also held by hydrogen interactions with the water ligand and the non-bridging phenoxide moiety of the L^{2-} ligand (Fig. S2, ESI[†]). On the other hand, the acetonitrile solvent molecules show

Table 1 Structural data for $\{Ni_3\}$ complexes with a bent arrangement and a $\mu-OR/\mu-syn$, *syn*-carboxylato bridge

| CSD code name | $Ni-Ni-Ni$ angle/degrees | Mean $Ni-O_{phenolate}$ bond distance/Å | $Ni-O_{phenolate}-Ni$ angle/degrees | Mean $Ni-O_{carboxylate}$ bond distance/Å | $RCOO-NiO_{ph}Ni$ torsion angle/degrees | Ref. |
|---------------|--------------------------|---|-------------------------------------|---|---|-----------|
| BENWEX | 131 | 2.066 | 124 | 2.048 | 30 | 7a |
| BENWIB | 132 | 2.063 | 123–125 | 2.037 | 32 | 7a |
| GAHTIU | 134 | 2.068 | 118 | 2.040 | 9 | 7b |
| KOMREL | 146 | 2.031 | 118 | 2.025 | 19 | 7c |
| PEMREH | 135 | 2.109 | 123 | 2.078 | 29 | 7d |
| ZEKREP | 149 | 2.012 | 118 | 2.019 | 33 | 7e |
| 1 | 146 | 2.040 | 117 | 2.029 | 24 | This work |

non-covalent short contact interactions with the free pivalic acid *tert*-butyl moieties and the methyl moieties of the L^{2-} ligand (Fig. S4, ESI†).

When looking in detail at the crystal structure packing, it is observed that the molecules of complex **1** run along the *c*-axis held by the previously described H-interaction. On the other hand, the acetonitrile and pivalic acid free molecules fill the channels in between (Fig. S5, ESI†). The closest intra-molecular Ni–Ni distance along this *c*-axis direction is 5.345(2) Å, longer than the intra-molecular Ni–Ni distance of 3.4800(13) Å.

Magnetic properties: experimental and quantum chemical calculations

In order to evaluate the spin ground state, as well as the magnitude and nature of the Ni(II)–Ni(II) exchange interactions, we performed DC magnetic measurements for complex **1**. The temperature dependence of magnetic susceptibility in the range 2–300 K shows a profile compatible with the dominant antiferromagnetic exchange interactions between the Ni(II) centres (Fig. 2).

At 300 K, the χT value of 4.204 cm³ K mol⁻¹ is consistent with the expected value for three isolated Ni(II) ions ($S = 1$) with a g value close to 2.3 of ca. 3.9 cm³ K mol⁻¹. This value smoothly drops to reach 3.783 cm³ K mol⁻¹ at 30 K where it abruptly diminishes to a final value of 1.719 cm³ K mol⁻¹ at 2 K. Of course, the single ion zero field splitting (ZFS) contributions from the Ni(II) sites are probably also contributing at low temperature in addition to the Ni(II)–Ni(II) antiferromagnetic exchange interaction. When looking at the reduced magnetization plots achieved in the range 2–10 K and up to a 70 kOe magnetic field, neither saturation is observed nor isotherms superposition (Fig. 2). This is in line with possible ZFS contributions and/or low-lying excited spin multiplets owing to weak exchange interactions.

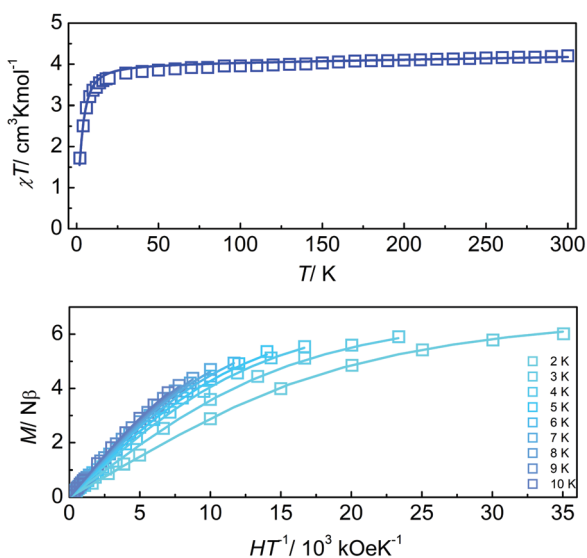
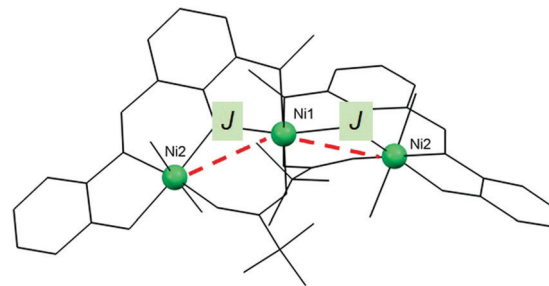


Fig. 2 Top: χT versus T data for complex **1** under a 1000 Oe magnetic field. Bottom: Reduced magnetization data for complex **1** in the range of 2–10 K under magnetic fields of up to 70 kOe. Open symbols: experimental data; full lines: simulations employing best fitting parameters with a negative D value, as described in the text.



Scheme 2 Exchange interactions considered in the spin Hamiltonian of eqn (1).

We performed a simultaneous data fitting of susceptibility and magnetization employing the PHI package.⁸ In order to reach a satisfactory agreement, the following spin Hamiltonian was required:

$$\hat{H} = g\beta B \sum_i \hat{S}_i - 2J(\hat{S}_1\hat{S}_2 + \hat{S}_2\hat{S}_3) + D \sum_i \hat{S}_{z,i}^2 \quad (1)$$

It includes a unique exchange interaction between the central and terminal Ni(II) ions (Scheme 2) (in agreement with the symmetry of complex **1**) as well as a unique axial local ZFS term (as including different ZFS terms for central and terminal sites would certainly result in over-parameterization problems).

This model proved to be the simplest, as well as the minimum required to provide a good agreement with the experimental data (Fig. 2 and Fig. S6, ESI†). Two sets of best fitting parameters were obtained: $g = 2.31$; $J = -0.32$ cm⁻¹; $D = -8.4$ cm⁻¹ and $g = 2.31$; $J = -0.48$ cm⁻¹; $D = 4.2$ cm⁻¹. A TIP (temperature independent paramagnetism) contribution of 600×10^{-6} cm³ K mol⁻¹ was also included. The data fitting residuals are lower for a negative D value, whereas at the same time a strong correlation is found between the J and D parameters (Fig. S7, ESI†). Despite the uncertainty around these parameter values, there is no doubt that ZFS dominates over the exchange interactions, precluding the strong exchange regime and making it harder to precisely determine the exchange interaction parameters. With a J value of around -0.5 cm⁻¹, a triplet ground state is found with a singlet at only 1 cm⁻¹ and the entire spin ladder closely packed in just 5 cm⁻¹.

In order to support the experimental results, we performed quantum chemical calculations of the spin Hamiltonian parameters (see Quantum chemical computations section). For the exchange interaction parameter we relied on the widely used broken-symmetry (BS) approach which we have successfully employed in related systems.^{2g,9} In the case of the computed g and ZFS tensors we performed CASSCF-SA-SOC (state averaged spin-orbit coupled) calculations based on all d^8 configuration microstates, over the crystallographic individual Ni(II) sites (central and terminal positions).

The calculated ZFS parameters, as well as the main values of the g -tensors show an excellent agreement with the experimental ones (Table 2), suggesting a negative value for D which was also presumed from the DC magnetic data fit residuals. The support from the quantum calculations of a sizeable D value, provides

Table 2 Magnetic data for $\{\text{Ni}_3\}$ complexes with a bent arrangement and a $\mu\text{-OR}/\mu\text{-syn}$, *syn*-carboxylate bridge

| CSD code name | Experimental SH parameters J , D/cm^{-1} | Computed SH parameters J , D/cm^{-1} | Computed J/cm^{-1} in the model OH-OH ₂ complex |
|---------------|---|---|---|
| BENWEX | — | — | — |
| BENWIB | — | — | — |
| GAHTIU | $g = 2.08$ $J = -0.85$ | $J = -0.72/-0.57$ | — |
| KOMREL | $g = 2.01$ $J = -1.28$ | $J = -2.85$ | — |
| PEMREH | — | — | — |
| ZEKREP | $g = 2.31$ $J = 0.51$ | $J = 0.49$ | $J = -0.54$ |
| 1 | $g = 2.31$ $J = -0.32 (-0.48)$ $D = -8.4 (4.2)$ | $g_{x,y,z} = (2.31 \ 2.32 \ 2.38)$ Ni(1) $g_{x,y,z} = (2.37 \ 2.32 \ 2.26)$ Ni(2) $J = -0.95$ $D = -10.0$ Ni(1) $ E/D = 0.02$ Ni(1) $D = -11.2$ Ni(2) $ E/D = 0.32$ Ni(2) | $J = -2.5$ |

robustness to the J exchange parameter value extracted, which is not a trivial task when the strong coupled regime is not valid ($J \ll D$).

For computation of the isotropic exchange interaction parameter, J , we employed two different BS states, obtained using the subsequent spin-flipping of the central and terminal Ni(II) spins (Fig. S8, ESI[†]). However, owing to the observed symmetry that makes both the terminal Ni(II) groups equivalent, it would have been sufficient with a unique BS state energy calculation. Hence, we obtained a mean calculated value (from both BS state energies), $J = -0.95 \text{ cm}^{-1}$, which is in good agreement with the experimental result (Table 2). Among the surveyed structural related bent Ni(II) complexes (Table 1), a small number were found in which the magnetic properties have been reported (Table 2). All of them also show an anti-ferromagnetic exchange interaction with a unique exception (KOMREL) that exhibits a ferromagnetic positive J value. Among the Ni(II) systems bearing a phenolate bridge, only the bis- μ_2 -phenolate ones have been deeply analysed through magneto-structural correlations. In these systems it has been shown that the Ni-O-Ni angle dominates the nature and magnitude of the exchange interaction. The critical angle for moving from a ferromagnetic to an antiferromagnetic interaction is close to 94° .^{21,22} In all complexes related to our reported compound **1** (Table 1), the Ni-O-Ni angle was well above this threshold, indicating an antiferromagnetic interaction. It must be stressed at this point that these complexes are not bis- μ_2 -phenolate, but single μ_2 -phenolate ones. In fact, if the values for the J magnitude between these two types of Ni(II) complex families are compared, a factor of ten is observed in favour of the bis-phenolate systems. Nevertheless, it seems reasonable to expect a similar Ni-O-Ni angle correlation for the single phenolate systems. Following this reasoning, all anti-ferromagnetic J parameters should be observed in the complexes shown in Table 2, however there is one case in which this is not true.

In order to gain a deeper insight into this singular instance we performed BS calculations over crystal structure geometries for all complexes in Table 2 for which the experimental magnetic data was available, at the same theory level employed for complex **1**. The obtained computed J parameters agree with the experimental ones. Thus, it is further confirmed the one case in

which the exchange interaction is ferromagnetic. Luckily, this compound is quite similar from a structural point of view to complex **1** offering us two examples with opposite J natures to compare.

No correlation was found between the J values and Ni-O_{phenolate} distances or the Ni-O_{phenolate}-Ni angles in all complexes shown in Table 2. Thus, we decided to test the carboxylate role in the exchange interaction parameter as the second bridging ligand. Clearly, it cannot be mediating an additional antiferromagnetic pathway, therefore it is feasible that it is exerting a counter-complementary effect. This effect is well known in Cu(II) complexes with the same combination of bridging ligands,¹⁰ but there are no reports for Ni(II) systems with the μ -phenoxo- μ -carboxylate bridge. In order to verify this hypothesis, we performed BS calculations on the two complexes (**1** and KOMREL, Table 2) substituting the bridging carboxylate ligand with aqua and hydroxo ligands placed at the same Ni-O bond distances (Fig. S9, ESI[†]). Using this strategy the unique bridging ligand is split into two independent ones disassembling any counter-complementary effect. Both of the calculated J parameters (Table 2) afford negative values supporting the feasibility of the counter-complementarity hypothesis, as the exchange coupling parameter becomes more negative when the carboxylate bridge is removed. Hence, the almost fixed Ni-O_{phenolate}-Ni angle at *ca.* $117\text{--}118^\circ$ observed in complexes in Table 1 provides an antiferromagnetic pathway (according to the double μ -phenolate existing correlations²¹) while the carboxylate bridge suppresses this contribution through a counter-complementarity effect. In the case of the complex which has an overall ferromagnetic interaction, this suppression must be improved in comparison with the other complexes showing anti-ferromagnetic interactions. This counter-complementarity role of the carboxylate bridge has also recently been observed in Cr(III) double μ -alkoxide- μ -carboxylate dinuclear systems.¹¹

From the inspection of the magnetic orbitals arising from the BS calculations (Fig. 3) it can be observed that the torsion angle between the plane containing the carboxylate -COO group and the plane containing the Ni-O_{phenolate}-Ni group, as well as the mean Ni-O_{carboxylate} bond distance, are the critical

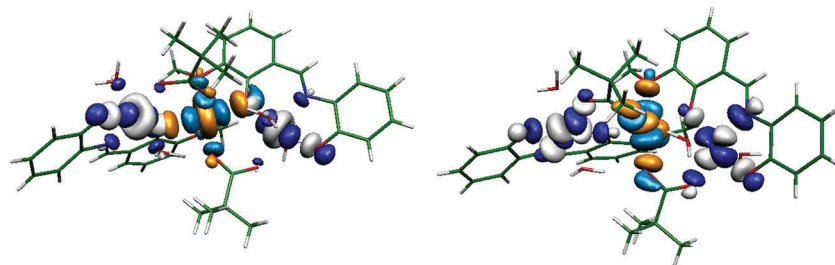
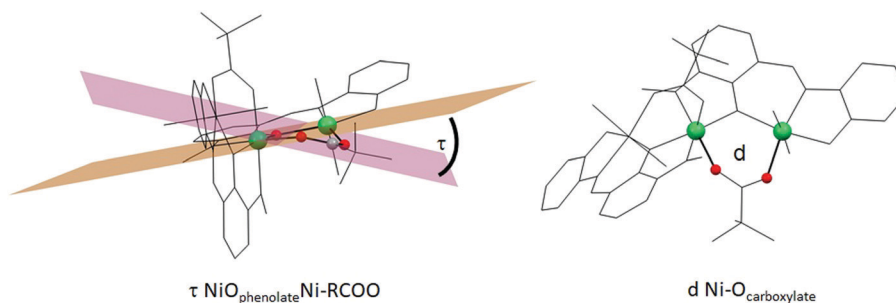


Fig. 3 Magnetic orbital iso-surface contours (0.02 a.u.) arising from COT for both BS calculations in complex **1**. The different colour combinations correspond to α - β pairs with overlapping that is significantly different from unity.



Scheme 3 Structural parameters influencing the counter-complementarity effect of the bridging carboxylate ligand.

parameters for the counter-complementarity contribution (Table 1 and Scheme 3).

In fact, these two parameters reasonably correlate with the observed tendency of the J values: the shorter Ni-O_{carboxylate} bonds, as well as the larger torsion angles indicate a ferromagnetic overall interaction (Fig. S10, ESI†). On the other hand, the anti-ferromagnetic contribution through the phenoxide bridge is explained in terms of a favourable overlap of at least one pair of magnetic orbitals. Nevertheless, many more examples with theoretical and experimental data must be accumulated before a magneto-structural correlation can be determined.

Conclusions

We have prepared and structurally characterized a novel {Ni₃} bent complex, bearing the double μ -phenoxide- μ -carboxylate bridge. Notably, very few reported examples sharing this motif can be found, and even less of them have been studied from the magnetic behaviour aspect; therefore, we decided to make a step forward in this direction. Combining DC magnetic experimental data, as well as quantum computations, we have shown that the nature of the weak exchange interaction between the Ni(II) ions seems to be established by counter-complementarity effects. Although the phenoxide ligand mediates a modest magnetic orbital overlap and promotes an antiferromagnetic pathway, the carboxylate bridge exerts counter-complementarity and favours ferromagnetic exchange. BS calculations support this idea and the variation of the main structural parameters (torsion angle and bond distances) around the carboxylate bridge suggest correlation with the nature of the J parameter. It is worth remarking

that the considerable single ion ZFS contribution of Ni(II) makes determination of the precise exchange interaction parameters a very challenging task. As the currently reported complexes feeding these results are still very scarce, more related novel complexes are needed to further test this preliminary hypothesis.

Experimental section

Material and physical measurements

The complex [Ni₂(μ -OH₂)(μ -piv)₂(piv)₂(Hpiv)₄], piv = trimethylacetate, was prepared following a previously reported procedure.¹² The ligand H₂L was prepared by standard reported procedures for this type of Schiff-base compound, by refluxing equimolar amounts of the starting materials *o*-vanillin and *o*-aminophenol in methanol and crystallizing the product by cooling.

All other chemicals were reagent grade and were used as received without further purification. Elemental analysis for C, H and N was performed using a Carlo Erba 1108 analyser.

Magnetic measurements were performed using a Quantum Design MPMS XL-7 SQUID magnetometer. All experimental magnetic data were corrected for the diamagnetism of the sample holders and for the constituent atoms (Pascal's tables). DC measurements were conducted from 2 to 300 K at 1 kOe and at 2 K in the range 1–70 kOe.

Preparation of complex Ni₃(L₂)(piv)₂(H₂O)₄·2Hpiv·CH₃CN (**1**)

0.1 g (0.105 mmol) of [Ni₂(μ -OH₂)(μ -piv)₂(piv)₂(Hpiv)₄] was dissolved at room temperature under an open atmosphere in 10 ml of acetonitrile. After complete dissolution resulting in a green solution, 0.025 g (0.105 mmol) of solid H₂L was added

and stirring was continued for one hour. The solution colour changed to brownish yellow. It was filtered to remove small amounts of undissolved materials and left standing undisturbed in a closed vial. After a week, yellow crystals suitable for X-ray diffraction (XRD) measurements were obtained. After picking one for single crystal XRD collection, the remaining crystals were filtered and washed with acetonitrile. After air drying, 0.034 g were obtained. Yield: 53%.

Anal. calcd for $C_{50}H_{71}N_3Ni_3O_{18}$ (1219.25 g mol⁻¹) C: 51.0, H: 6.1, N: 3.6 found: C: 51.1, H: 5.9, N: 4.4.

DC magnetic measurements

X-ray structure determination. The crystal structure of compound **1** was determined with an Oxford Xcalibur, Eos, Gemini CCD area-detector diffractometer using graphite-monochromated Mo-K α radiation ($\lambda = 0.71069 \text{ \AA}$) at 298 K. Crystals were directly obtained from the synthetic procedure. Data was corrected for absorption with CrysAlisPro, Oxford Diffraction Ltd, Version 1.171.33.66, applying an empirical absorption correction using spherical harmonics, implemented in the SCALE3 ABSPACK scaling algorithm.¹³ The structures were solved using direct methods with SHELXT¹⁴ and refined by full-matrix least-squares on F^2 with SHELXL-2014¹⁵ under the WinGX platform.¹⁶ Hydrogen atoms were added geometrically and refined as riding atoms with a uniform value of U_{iso} , with the exception of aqua ligands and the pivalic acid solvent molecule, whose H atoms were located in the difference map and further refined with O–H constrained distances. The solvent acetonitrile

molecule appears to be disordered around two positions related by a crystallographic C_2 axis. It was then refined with 0.5 occupancy numbers.

Final crystallographic data and values of R_1 and wR are listed in Table 3. CCDC 1938756 contains the supplementary crystallographic data for this paper.†

Quantum chemical calculations

For the computation of the exchange interaction J parameters, the ORCA program package¹⁷ was employed. Single point calculations for the high-spin state (HS) and the broken-symmetry (BS) states at the X-ray geometry were carried out at the B3LYP level of density functional theory (DFT) employing the def2-TZVP Ahlrichs basis set for all atoms and taking advantage of the RI (resolution of identity) approximation. The self-consistent field (SCF) calculations were of the spin-polarized type and were tightly converged ($10^{-7} E_h$ in energy, 10^{-6} in the density change and 10^{-6} in the maximum element of the DIIS error vector).

The methodology applied here relies on the BS formalism, originally developed by Noodleman for SCF methods,¹⁸ which involves a variational treatment within the restrictions of a single spin-unrestricted Slater determinant built upon using different orbitals for different spins. This approach has been later applied within the frame of DFT.¹⁹ The HS and BS energies were then combined to estimate the exchange coupling parameter J involved in the widespread used Heisenberg–Dirac–van

Table 3 Crystallographic data for complex **1**

| | 1 |
|--|--|
| Empirical formula | $C_{50}H_{71}N_3Ni_3O_{18}$ |
| Formula weight | 1178.22 |
| T (K) | 298 (2) |
| Crystal system | Monoclinic |
| Space group | $C_{2/c}$ |
| a (Å) | 17.893(3) |
| b (Å) | 16.511(2) |
| c (Å) | 21.476(4) |
| α (°) | 90 |
| β (°) | 110.56(2) |
| γ (°) | 90 |
| V (Å ³) | 5941(2) |
| Z | 4 |
| D_{calc} (mg m ⁻³) | 1.317 |
| Absorption coefficient (mm ⁻¹) | 1.008 |
| $F(000)$ | 2480 |
| λ (Å) | 0.71069 |
| θ range data collection (°) | 3.64–27.0 |
| Index ranges | $-22 \leq h \leq 19$ $-19 \leq k \leq 20$ $-27 \leq l \leq 26$ |
| Reflections collected/unique | 13 797/5905 |
| R_{int} | 0.0761 |
| Observed reflections [$I > 2\sigma(I)$] | 3591 |
| Completeness (%) | 93.2 |
| Maximum/minimum transmission | 1.000/0.361 |
| Data/restraints/parameters | 5905/22/364 |
| Goodness-of-fit (GOF) on F^2 | 1.023 |
| Final R -index [$I > 2\sigma(I)$]/all data | 0.0761/0.2568 |
| wR index [$I > 2\sigma(I)$]/all data | 0.2030/0.2568 |
| Largest peak and hole (e Å ⁻³) | 1.166 and -0.459 |
| Weights, w | $1/[\sigma^2(F_o^2) + (0.1399P)^2 + 0.6906P]$ where $P = (F_o^2 + 2F_c^2)/3$ |

Vleck Hamiltonian. We used the method proposed by Ruiz and co-workers,²⁰ in which the following equation is applied:

$$E_{\text{BS}} - E_{\text{HS}} = 2J_{12}(2S_1S_2 + S_1), \text{ with } S_2 < S_1 \quad (2)$$

We have calculated the different spin topologies for the BS nature (Fig. S8, ESI†) by alternately flipping spin on the different metal sites. The exchange coupling constants J_i were obtained after considering the individual pair-like components spin interactions involved in the description of the different BS states by solving a set of linear equations. In order to visualize the magnetic orbitals involved in the exchange interactions we performed the corresponding orbital transformations (COT) over the BS solutions²¹ as implemented in ORCA.

To compute the local g and ZFS tensors, the MOLCAS package (as the MOLCAS@UU version) was employed.²² The calculations of these parameters for the two different Ni(II) sites in the trinuclear complex were performed by replacing the remaining Ni(II) sites with the diamagnetic Zn(II) cation. We performed these computations at the complete active space self-consistent field (CASSCF) level, and the spin-orbit coupling (SOC) was introduced in a second step using the spin orbital restricted-active-space state-interaction (SO-RASSI) method. We performed a states-average approach including the full d^8 microstates, 10 triplets and 15 singlets in the SO-RASSI step. For the CASSCF calculation, the active space contained eight electrons in five orbitals (the five 3d orbitals). Relativistic atomic natural orbital (ANO-RCC) basis sets were used with the following contraction scheme: 7s6p4d3f2g1h (VQZP) for Ni and Zn, 4s3p2d (VTZ) for O and N, 3s2p (VDZ) for C and 2s (VDZ) for H. Final g and ZFS tensors were obtained through the SINGLE-ANISO MOLCAS routine.

Conflicts of interest

There are no conflicts of interest to declare.

Acknowledgements

We gratefully acknowledge UBA, ANPCYT and CONICET for funding resources. PA is a staff member of CONICET. The authors gratefully acknowledge computing time granted on the supercomputer Mogon at Johannes Gutenberg University Mainz (hpc.uni-mainz.de).

References

- J. Ferrando-Soria, J. Vallejo, M. Castellano, J. Martínez-Lillo, E. Pardo, J. Cano, I. Castro, F. Lloret, R. Ruiz-García and M. Julve, *Coord. Chem. Rev.*, 2017, **339**, 17–103.
- (a) V. H. Crawford, H. W. Richardson, J. R. Wasson, D. J. Hodgson and W. E. Hatfield, *Inorg. Chem.*, 1976, **15**, 2107–2110; (b) J. Glerup, D. J. Hodgson, E. Pedersen, A. Haaland, B. E. R. Schilling, R. Seip and K. Taugbøl, *Acta Chem. Scand., Ser. A*, 1983, **37**, 161–164; (c) S. Sasmal, S. Hazra, P. Kundu, S. Dutta, G. Rajaraman, E. C. Sañudo and S. Mohanta, *Inorg. Chem.*, 2011, **50**, 7257–7267; (d) N. Berg, T. Rajeshkumar, S. M. Taylor, E. K. Brechin, G. Rajaraman and L. F. Jones, *Chem. – Eur. J.*, 2012, **18**, 5906–5918; (e) W. P. Barros, R. Inglis, G. S. Nichol, T. Rajeshkumar, G. Rajaraman, S. Piligkos, H. O. Stumpf and E. K. Brechin, *Dalton Trans.*, 2013, **42**, 16510; (f) J. P. S. Walsh, S. Sproules, N. F. Chilton, A. Barra, G. A. Timco, D. Collison, E. J. L. McInnes and R. E. P. Winpenny, *Inorg. Chem.*, 2014, **53**, 8464–8472; (g) A. V. Funes, L. Carrella, L. Sorace, E. Rentschler and P. Alborés, *Dalton Trans.*, 2015, **44**, 2390–2400; (h) E. A. Suturina, D. Maganas, E. Bill, M. Atanasov and F. Neese, *Inorg. Chem.*, 2015, **54**, 9948–9961; (i) I. Oyarzabal, J. Ruiz, A. J. Mota, A. Rodríguez-Diéguez, J. M. Seco and E. Colacio, *Dalton Trans.*, 2015, **44**, 6825–6838; (j) F. Torić, G. Pavlović, D. Pajić, M. Cindrić and K. Zadro, *CrystEngComm*, 2018, **20**, 3917–3927; (k) M. K. Singh and G. Rajaraman, *Inorg. Chem.*, 2019, **58**, 3175–3188; (l) F. Torić, G. Pavlović, D. Pajić, T. Hrenar, K. Zadro and M. Cindrić, *Inorg. Chim. Acta*, 2019, **484**, 457–463; (m) S. M. Gorun and S. J. Lippard, *Inorg. Chem.*, 1991, **30**, 1625–1630; (n) K. K. Nanda, L. K. Thompson, J. N. Bridson and K. Nag, *J. Chem. Soc., Chem. Commun.*, 1994, **8**, 1337–1338; (o) M. A. Halcrow, J. S. Sun, J. C. Huffman and G. Christou, *Inorg. Chem.*, 1995, **34**, 4167–4177; (p) H. Weihe and H. U. Güdel, *J. Am. Chem. Soc.*, 1998, **120**, 2870–2879; (q) T. K. Karmakar, B. K. Ghosh, A. Usman, H. K. Fun, E. Rivière, T. Mallah, G. Aromí and S. K. Chandra, *Inorg. Chem.*, 2005, **44**, 2391–2399; (r) S. Triki, C. J. Gómez-García, E. Ruiz and J. Sala-Pala, *Inorg. Chem.*, 2005, **44**, 5501–5508; (s) R. Inglis, L. F. Jones, C. J. Milios, S. Datta, A. Collins, S. Parsons, W. Wernsdorfer, S. Hill, S. P. Perlepes, S. Piligkos and E. K. Brechin, *Dalton Trans.*, 2009, 3403; (t) R. Costa, I. de, P. R. Moreira, S. Youngme, K. Siriwong, N. Wannarit and F. Illas, *Inorg. Chem.*, 2010, **49**, 285–294.
- D. Gatteschi, R. Sessoli and J. Villain, *Molecular Nanomagnets*, Oxford University Press, 2006.
- O. Kahn, *Molecular Magnetism*, Wiley-VCH Verlag GmbH & Co. KGaA, 1993.
- (a) K. C. Mondal, G. E. Kostakis, Y. Lan, W. Wernsdorfer, C. E. Anson and A. K. Powell, *Inorg. Chem.*, 2011, **50**, 11604–11611; (b) H. Ke, L. Zhao, Y. Guo and J. Tang, *Inorg. Chem.*, 2012, **51**, 2699–2705; (c) S. Bag, P. K. Bhaumik, S. Jana, M. Das, P. Bhowmik and S. Chattopadhyay, *Polyhedron*, 2013, **65**, 229–237; (d) S. Saha, S. Pal, C. J. Gómez-García, J. M. Clemente-Juan, K. Harms and H. P. Nayek, *Polyhedron*, 2014, **74**, 1–5; (e) H. Ke, S. Zhang, W. Zhu, G. Xie and S. Chen, *J. Coord. Chem.*, 2015, **68**, 808–822; (f) K. Griffiths, C. W. D. Gallop, A. Abdul-Sada, A. Vargas, O. Navarro and G. E. Kostakis, *Chem. – Eur. J.*, 2015, **21**, 6358–6361; (g) K. Griffiths, P. Kumar, J. D. Mattock, A. Abdul-Sada, M. B. Pitak, S. J. Coles, O. Navarro, A. Vargas and G. E. Kostakis, *Inorg. Chem.*, 2016, **55**, 6988–6994; (h) K. Griffiths, V. N. Dokorou, J. Spencer, A. Abdul-Sada, A. Vargas and G. E. Kostakis, *CrystEngComm*, 2016, **18**, 704–713; (i) S. Saha, S. Jana, S. Gupta, A. Ghosh and H. P. Nayek, *Polyhedron*, 2016, **107**, 183–189;

- (j) K. Griffiths, A. Escuer and G. E. Kostakis, *Struct. Chem.*, 2016, **27**, 1703–1714.
- 6 C. R. Groom, I. J. Bruno, M. P. Lightfoot and S. C. Ward, *Acta Crystallogr., Sect. B: Struct. Sci., Cryst. Eng. Mater.*, 2016, **72**, 171–179.
- 7 (a) H. Adams, D. E. Fenton and P. E. McHugh, *Inorg. Chem. Commun.*, 2004, **7**, 147–150; (b) Y. Y. Hui, H. M. Shu, H. M. Hu, J. Song, H. L. Yao, X. Le Yang, Q. R. Wu, M. L. Yang and G. L. Xue, *Inorg. Chim. Acta*, 2010, **363**, 3238–3243; (c) X. Qin, Y. Ji, Y. Gao, L. Yan, S. Ding, Y. Wang and Z. Liu, *Z. Anorg. Allg. Chem.*, 2014, **640**, 462–468; (d) C.-Y. Li, Y.-C. Su, C.-H. Lin, H.-Y. Huang, C.-Y. Tsai, T.-Y. Lee and B.-T. Ko, *Dalton Trans.*, 2017, **46**, 15399–15406; (e) M. Liu, H. Yu, Y. Wang and Z. Liu, *Inorg. Chem. Commun.*, 2017, **86**, 281–284.
- 8 N. F. Chilton, R. P. Anderson, L. D. Turner, A. Soncini and K. S. Murray, *J. Comput. Chem.*, 2013, **34**, 1164–1175.
- 9 (a) P. Alborés, J. Seeman and E. Rentschler, *Dalton Trans.*, 2009, 7660–7668; (b) P. Alborés and E. Rentschler, *Polyhedron*, 2009, **28**, 1912–1916; (c) P. Alborés and E. Rentschler, *Inorg. Chem.*, 2010, **49**, 8953–8961; (d) P. Alborés, C. Plenck and E. Rentschler, *Inorg. Chem.*, 2012, **51**, 8373–8384; (e) I. C. Lazzarini, L. Carrella, E. Rentschler and P. Alborés, *Polyhedron*, 2012, **31**, 779–788; (f) P. Alborés and E. Rentschler, *Dalton Trans.*, 2013, **42**, 9621–9627; (g) I. C. Lazzarini, A. V. Funes, L. Carrella, L. Sorace, E. Rentschler and P. Alborés, *Eur. J. Inorg. Chem.*, 2014, 2561–2568; (h) C. Sarto, M. Rouzières, J. L. Liu, H. Bamberger, J. Van Slageren, R. Clérac and P. Alborés, *Dalton Trans.*, 2018, **47**, 17055–17066.
- 10 (a) G. Christou, E. Libby, K. Folting, J. C. Huffman, R. J. Webb, D. N. Hendrickson and S. P. Perlepes, *Inorg. Chem.*, 1990, **29**, 3657–3666; (b) K. S. Bürger, P. Chaudhuri and K. Wieghardt, *J. Chem. Soc., Dalton Trans.*, 1996, **1**, 247–248; (c) H. Nie, S. M. J. Aubin, M. S. Mashuta, R. A. Porter, J. F. Richardson, D. N. Hendrickson and R. M. Buchanan, *Inorg. Chem.*, 2002, **35**, 3325–3334.
- 11 H. W. L. Fraser, L. Smythe, S. Dey, G. S. Nichol, S. Piligkos, G. Rajaraman and E. K. Brechin, *Dalton Trans.*, 2018, **47**, 8100–8109.
- 12 G. Chaboussant, R. Basler, H. Güdel, S. Ochsenein, A. Parkin, S. Parsons, G. Rajaraman, A. Sieber, A. A. Smith, G. A. Timco and R. E. P. Winpenny, *Dalton Trans.*, 2004, 2758–2766.
- 13 SCALE3 ABSPACK: empirical absorption correction, CrysAlis – Software package, 2006.
- 14 G. M. Sheldrick, *Acta Crystallogr., Sect. A: Found. Adv.*, 2015, **71**, 3–8.
- 15 G. M. Sheldrick, *Acta Crystallogr., Sect. A: Found. Crystallogr.*, 2008, **64**, 112–122.
- 16 L. J. Farrugia, *J. Appl. Crystallogr.*, 2012, **45**, 849–854.
- 17 F. Neese, *Wiley Interdiscip. Rev.: Comput. Mol. Sci.*, 2012, **2**, 73–78.
- 18 L. Noodleman, *J. Chem. Phys.*, 1981, **74**, 5737–5743.
- 19 L. Noodleman and E. J. Baerends, *J. Am. Chem. Soc.*, 1984, **106**, 2316–2327.
- 20 (a) E. Ruiz, J. Cano, S. Alvarez and P. Alemany, *J. Comput. Chem.*, 1999, **20**, 1391–1400; (b) E. Ruiz, A. Rodríguez-Fortea, J. Cano, S. Alvarez and P. Alemany, *J. Comput. Chem.*, 2003, **24**, 982–989.
- 21 F. Neese, *J. Phys. Chem. Solids*, 2004, **65**, 781–785.
- 22 F. Aquilante, J. Autschbach, R. K. Carlson, L. F. Chibotaru, M. G. Delcey, L. De Vico, I. Fdez. Galván, N. Ferré, L. M. Frutos, L. Gagliardi, M. Garavelli, A. Giussani, C. E. Hoyer, G. Li Manni, H. Lischka, D. Ma, P. Å. Malmqvist, T. Müller, A. Nenov, M. Olivucci, T. B. Pedersen, D. Peng, F. Plasser, B. Pritchard, M. Reiher, I. Rivalta, I. Schapiro, J. Segarra-Martí, M. Stenrup, D. G. Truhlar, L. Ungur, A. Valentini, S. Vancioillie, V. Veryazov, V. P. Vysotskiy, O. Weingart, F. Zapata and R. Lindh, *J. Comput. Chem.*, 2016, **37**, 506–541.